

1 **Id4 is required for normal ependymal cell development**

2
3 **Brenda Rocamonde^{1#*}, Vicente Herranz-Pérez^{2,3}, Jose-Manuel Garcia-Verdugo² and**
4 **Emmanuelle Huillard^{1*}**

5
6 ¹Sorbonne Université, Institut du Cerveau - Paris Brain Institute - ICM, Inserm, CNRS, APHP,
7 Paris, France

8 ²Laboratory of Comparative Neurobiology, Institute Cavanilles, University of Valencia,
9 CIBERNED, 46980 Paterna, Valencia, Spain

10 ³Predepartamental Unit of Medicine, Faculty of Health Sciences, University Jaume I, Castelló de la
11 Plana, Spain

12 [#]current address: International Center for Research in Infectiology, Retroviral Oncogenesis
13 Laboratory, INSERM U1111 - Université Claude Bernard Lyon 1, CNRS, UMR5308, Ecole
14 Normale Supérieure de Lyon, Université Lyon, Lyon, France, Equipe labélisée par la Fondation
15 pour la Recherche Médicale, Labex Ecofect.

16 *** Authors for correspondence:**

17 Emmanuelle Huillard: emmanuelle.huillard@icm-institute.org

18 Brenda Rocamonde: brenda.rocamonde-esteve@ens-lyon.fr

19
20
21
22 **Keywords:** brain, ependymal cell, ID4, transcription factor, brain development, cilia.

23 **Abstract**

24
25 Ependymal cells are radial glia-derived multiciliated cells lining the lateral ventricles of the brain
26 and spinal cord. Correct development and coordinated cilia beating is essential for proper
27 cerebrospinal fluid flow (CSF) and neurogenesis modulation. Dysfunctions of ependymal cells were
28 associated with transcription factor deregulation. Here we provide evidence that the transcriptional
29 regulator Id4 is involved in ependymal cell development and maturation. We observed that *Id4*-
30 deficient mice display altered ependymal cytoarchitecture, decreased ependymal cell number,
31 altered CSF flow and enlarged ventricles. Our findings open the way for a potential role of Id4 in
32 ependymal cell development and/or motor cilia function.

33 34 35 **1 Introduction**

36 Ependymal cells are multiciliated epithelial cells organized in a monolayer lining the lateral
37 ventricles (LV) (Doetsch et al., 1997). A subpopulation of radial glia-derived B1 astrocytes present
38 an apical membrane extending a primary cilia that contacts the ventricle (Doetsch et al., 1999;
39 Merkle et al., 2004). Monociliated B1 astrocytes and multiciliated ependymal cells are organized
40 within the neurogenic regions of the ventricle wall forming unique pinwheel structures (Mirzadeh et
41 al., 2008).

42 Ependymal cells are derived from radial glia during embryogenesis between embryonic day 14
43 (E14) and E16, while maturation occurs later during the first postnatal week. Ependymal cells are
44 born as monociliated epithelial cells (9+0) and their maturation as multiciliated cells (9+2) happens
45 during postnatal day 0 (P0) and P10 (Spassky et al., 2005). It was reported that rotational and
46 translational orientation of basal bodies (BB) are determinant factors of planar cell polarity (PCP)
47 and correlate with CSF flow direction. The coordinated ependymal cell beating is responsible for
48 the correct cerebrospinal fluid (CSF) flow through the ventricular system. CSF flow disruption due
49 to ependymal cell malfunction can lead to hydrocephaly (Taulman et al., 2001) and could impact
50 neuroblast migration towards the olfactory bulb (OB) (Sawamoto et al., 2006).

51 Factors controlling differentiation and maturation of ependymal cells are not well characterized. It
52 is known that the forkhead transcription factor FOXJ1 is necessary for ependymal cell
53 differentiation from radial glial cells and ciliogenesis (Jacquet et al., 2009). The homeobox factor
54 SIX3 and the transcription factor nuclear factor IX (NFIX) are also involved in ependymal cell
55 development and maturation (Lavado and Oliver, 2011; Vidovic et al., 2018). More recently, it was
56 demonstrated that Geminin and its antagonist GemC1, which are regulators of DNA replication, can
57 determinate the proportion of ependymal cells and neural stem cells (Ortiz-Álvarez et al., 2019).
58 Inhibitor of DNA-binding 4 protein (ID4) is a helix-loop-helix (HLH) protein, acting as a binding
59 partner and modulator of bHLH transcription factors. During embryonic development, ID4 plays an
60 important role in the development of the central nervous system, regulating neural stem cell
61 proliferation and differentiation. ID4-deficient mice present premature differentiation and
62 compromised cell cycle transition of early progenitor cells resulting in smaller brain (Bedford et al.,
63 2005; Yun et al., 2004). However, the role of ID4 in ependymal cell development and maturation
64 from radial glia cells has not yet been addressed. Here we show that ID4 is necessary for correct
65 development of the LV epithelium and for correct ependymal cell maturation. Absence of ID4
66 during crucial stages of neural fate decision leads to defective ependymal cell development,
67 disrupted planar cell polarity (PCP) and hydrocephalus. Our data suggest for the first time a role for
68 ID4 in ependyma development and function.

69
70

71 **2 Experimental Procedures**

72 **2.1 Animals.** Mice were housed, bred and treated in an authorized facility (agreement number
73 A751319). All experimental procedures involving mice have been approved by the French Ministry
74 of Research and Higher Education (project authorization number 3572-201601 0817294743 v5).
75 C57BL/6J (Charles River laboratories) and *Id4*^{-/-} (Yun et al., 2004; PMID: 15469968) mice were
76 used at 2-3 months of age. *Glast::CreERT2* (Mori et al., 2006) mice bred to *Id4fl* mice (Best et al.,
77 2014) to obtain *Glast::CreERT2;Id4fl* mice. To induce *Id4* deletion, a solution of 60 mg/kg of
78 tamoxifen and 20mg/kg of progesterone diluted in corn oil was administered by oral gavage to
79 pregnant females harvesting embryos at embryonic day 15 (E15). Pups were then obtained at P0 or
80 P10 for wholmount dissection.

81

82 **2.2 Wholmount dissection and immunolabelling.** Animals were sacrificed by cervical
83 dislocation. Then, brain was dissected and the whole ventricular-subventricular zone (V-SVZ) was
84 microdissected as described in Mirzadeh *et al.* (Mirzadeh et al., 2010). Fresh tissue was either fixed
85 with 4% paraformaldehyde (PFA; Electron Microscopy Sciences, EMS) and incubated with anti-
86 ZO-1 (1:200, Thermo Fisher Scientific ref. 402200); acetylated tubulin (6-11B, 1:200, Sigma
87 Aldrich ref. T6793) primary antibodies; or fixed with cold 70% ethanol for 10 min and incubated
88 with the anti-gamma tubulin (GTU88, 1:200, Abcam ref. ab11361) primary antibody. Samples were
89 incubated with secondary antibodies Alexa Fluor™ 488 and 596 (1:1000, Life Science
90 Technologies). Then wholmount sections were microdissected and mounted with fluoromount
91 (Sigma, ref F4680). Planar cell polarity (PCP) was determined by the altered orientation of the basal
92 bodies (BB) with respect of the cell wall as described in Mirzadeh *et al.* (Mirzadeh et al., 2010).

93

94 **2.3 Immunofluorescence.** Animals were anesthetized with 1 g/Kg sodium pentobarbital (Euthasol)
95 and intracardially perfused with 4% PFA in NaCl 0.9% solution. Brains were dissected and post-
96 fixed in the same solution for 24 h. Fifty micron coronal sections were obtained using a vibratome
97 (Microm). Floating sections were permeabilized with 0.01 M phosphate buffer saline (PBS)
98 containing 0.1% Triton X-100 for 5 min, blocked for 1 hour with 10% Normal Goat Serum
99 (Eurobio Ingen, cat CAECHV00-0U) in PBS-Triton 0.1% (blocking buffer) at room temperature
100 RT and incubated overnight at 4°C with rabbit anti-ID4 (1:1000, Biocheck ref. BCH-9/82-12) and

101 mouse anti-FOXJ1 (1:500, eBiosc 14-9965-82) antibodies diluted in blocking buffer. Then samples
102 were incubated with anti-mouse Alexa Fluor™ 488 and anti-rabbit Alexa Fluor™ 596 secondary
103 antibodies (1:1000, Life Science Technologies) diluted in blocking buffer. Finally, sections were
104 incubated in DAPI solution for nuclear staining (Invitrogen, cat D3571) and mounted on glass-
105 slides with Fluoromount (Sigma, cat F4680).

106
107 **2.4 Electron microscopy and immunogold staining.** For scanning electron microscopy, whole-
108 mount preparations of the lateral wall of lateral ventricles of four animals per group were dissected
109 and fixed with 2 % PFA + 2.5 % glutaraldehyde (EMS) in 0.1 M phosphate buffer (PB) and post-
110 fixed with 1% osmium tetroxide (EMS) in phosphate buffer (PB) for 2 hr, rinsed with deionized
111 water, and dehydrated first in ethanol then with CO₂ by critical point drying method. The samples
112 were coated with gold/palladium alloy by sputter coating. The surface of the lateral wall was
113 studied under a Hitachi S-4800 scanning electron microscope using Quantax 400 software (Bruker
114 Corporation) for image acquisition.

115 For pre-embedding immunogold staining, mice were perfused with 4% PFA in 0.1 M PB. Brains
116 were postfixed in in the same fixative solution overnight at 4 °C and sectioned into 50 µm
117 transversal sections using a vibratome. Pre-embedding immunogold staining with rabbit anti-ID4
118 antibody (1:500; Biocheck) were carried out as previously described (Sirerol-Piquer et al., 2012).
119 Sections were contrasted with 1% osmium tetroxide, 7% glucose in 0.1 M PB and embedded in
120 Durcupan epoxy resin. Subsequently, 1.5 µm semithin sections were prepared, lightly stained with
121 1% toluidine blue and selected at the light microscope level. Selected levels were cut into 60-80 nm
122 ultrathin sections. These sections were placed on Formvar-coated single-slot copper grids (Electron
123 Microscopy Sciences) stained with lead citrate and examined at 80 kV on a FEI Tecnai G² Spirit
124 (FEI Company) transmission electron microscope equipped with a Morada CCD digital camera
125 (Olympus).

126

127 **2.5 Image acquisition and analysis**

128 Fluorescent images were obtained using a Zeiss ApoTome 2 Microscope or Olympus Confocal
129 microscope FV1000. Images were analysed using ImageJ software.

130

131 **2.6 Statistical analysis.** Statistical analysis was performed using GraphPad Prism 6. Unless
132 otherwise indicated in the figure legends, non-parametric Mann-Whitney test was used to compare
133 experimental and control groups. Values are expressed as mean ± standard deviation.

134

135

136 **3 Results**

137 **3.1 ID4 is expressed in ependymal cells from the LV**

138 We performed ID4 immunolabelling on wholemount preparations of the LV of adult C57BL/6J
139 mice (Figure 1A). We detected the expression of ID4 protein in ependymal cells as can be observed
140 by co-localization with FOXJ1 protein (Figure 1B). To confirm this observation, we performed
141 immuno-gold labelling for the ID4 protein in ultrathin sections from the V-SVZ. Several cell types,
142 such as B1 astrocytes and progenitor stem cells were positive for ID4-immungold. In addition, ID4
143 labelling was detected in ependymal cells lining the LV confirming our immunofluorescence results
144 (arrowheads in Figure 1C).

145

146 **3.2 *Id4*^{-/-} mice display defects in LV development and ependymal cells function**

147 In order to investigate the role of ID4 in ependymal cells, we analysed the V-SVZ of *Id4*^{-/-} mice
148 (*Id4*KO) (Yun et al., 2004). *Id4*KO mice consistently displayed enlarged ventricles (Figure 2A-B).
149 This was associated with thinning of the ventricular wall and stretching of the ependymal cells, as
150 observed by light microscopy in toluidine blue-stained semithin sections (Figure 2C). Scanning

151 electron microscopy of wholemount preparations revealed the absence of adhesion point –the area
152 of the lateral and medial ventricle wall that adheres to each other– in *Id4*^{-/-} mice (Figure 2D). In
153 addition, we observed that ependymal cell density was decreased in all three rostral, central and
154 caudal areas of the ventricle wall.

155 To confirm a decrease in ependymal cell density, we performed immunofluorescent staining on
156 wholemount preparations of the cell wall (labelling tight junctions with ZO-1 antibody) and cilia
157 (acetylated tubulin, 6-11B) in WT and *Id4*KO mice (Figure 3A). The density of ependymal cells
158 was significantly decreased in *Id4*KO mice together with an increase in the cell surface when
159 compared the same regions (Figure 3B-C). To investigate whether altered ependyma in *Id4*KO
160 brains might lead to altered CSF flow, we evaluated planar cell polarity of ependymal cells (PCP)
161 by measuring cilia basal bodies (BB) orientation (Mirzadeh et al., 2010). Basal bodies were labelled
162 with anti- γ -tubulin (GTU88) antibody and its orientation was determined relative to the ependymal
163 cell wall labelled anti-ZO1 antibody. We noticed that the organization of BB patches was altered in
164 the *Id4*KO mice, with a significant decrease of the median orientation (Figure 3D,E).

165

166 **3.3 *Id4* deletion during embryogenesis impacts on ependymal cell development**

167 Ependymal cells differentiate from radial glia cells at E14-16 and maturation occurs from caudal to
168 rostral orientation during the first postnatal weeks (Spassky et al., 2005), where the primary cilium
169 is replaced by multiple motile cilia (9+2) (Mirzadeh et al., 2010). To evaluate whether *ID4* was
170 involved in ependymal cell differentiation and/or maturation we induced *Id4* deletion in
171 *GlastCreERT2-Id4flox (Id4cKO)* mice at E15 and analysed their phenotype at P0 to evaluate
172 differentiation and at P10 to analyse maturation (Figure 4A). We performed immunofluorescence
173 for γ -tubulin (GTU88) to identify the BB and for ZO1. The defects in ependymal cell maturation
174 were already present at P0 but were more evident at P10 (Figure 4B). In addition, the number of
175 ependymal cells seemed to be decreased already at P0, suggesting that *Id4* may be involved in
176 differentiation of ependymal cells at embryonic stages. Quantification of the number of ependymal
177 cells showed a significant decrease in *Id4cKO* in rostral regions at P0 (Figure 4C). In addition,
178 evaluation of the presence of matured ependymal cells at P10 showed a decline in *Id4cKO* LV,
179 although it did not reach statistical significance. Together, our data suggest that *Id4* may be
180 important for ependymal cell maturation and correct cilia development.

181

182

183 **4 Discussion**

184 *ID4* plays an essential role in correct neural cell differentiation and maturation during
185 embryogenesis (Yun et al., 2004; Bedford et al., 2005). In this work, we present evidence that *ID4*
186 might also be important for development and maturation of ependymal cells from radial glial cells.
187 First, we describe for the first time that *ID4* protein is expressed in ependymal cells. Absence of
188 *ID4*, initiated at early stages of brain development, resulted in altered ependymal cell layer
189 cytoarchitecture, decreased ependymal cell numbers and enlarged ventricles as a consequence. The
190 absence of adhesion point was also a constant in *Id4*KO mice and was already reported to be linked
191 to hydrocephalus in other mutants, such as *KIF3A*-deficient mice (Mirzadeh et al., 2010). Early
192 inactivation of *Id4* at E15 during differentiation of ependymal cells from radial glial cells resulted in
193 decreased number of ependymal cells, suggesting that *ID4* may be important in ependymal cell
194 determination from radial glial cells. Defects in differentiation from radial glial cells were also
195 observed when the forkhead transcription factor *FOXJ1* was absent (Jacquet et al., 2009). *GemC1* –
196 a regulator of the DNA replication– was another factor playing an important role in the ependymal
197 cell-neural stem cell balance (Ortiz-Álvarez et al., 2019).

198 In addition to a defective differentiation, our findings suggest that *ID4* may also be involved in
199 ciliogenesis. Delayed ciliogenesis was also detected in ependymal cells at P10 when *Id4* was
200 deleted. Another transcription factors involved in ciliogenesis were *FOXJ1* and *NFIX* (Jacquet et

201 al., 2009; Vidovic et al., 2018). Decreased number and delayed maturation of ependymal cell
202 beating capacity could lead to disrupted CSF flow dynamics early during brain development and
203 accumulation of CSF. Accumulation of CSF within the brain ventricles due to defect in ependymal
204 cell development is one of the mechanisms responsible of hydrocephalus (Ibañez-Tallon et al.,
205 2004). Despite complete cilia development in ependymal cells, PCP seemed to be affected by the
206 absence of Id4. This could suggest a potential role of Id4 in centrosome organization or cilia
207 motility. Malfunction in ependymal cell beating activity can impair CSF clearance and cause
208 excessive accumulation within the ventricles leading to hydrocephalus as a result of increased
209 pressure. On the other hand, CSF flow dynamics can also impact neural stem cell (NSC)
210 proliferation and neuroblast migration towards the olfactory bulb. Several studies have reported that
211 the NSC's primary cilium works as an "antenna" sensing the changes in CSF flow (Silva-Vargas et
212 al., 2016). CSF flow generates protein gradients contributing with vector information for migratory
213 neuroblasts (Sawamoto et al., 2006). Therefore, disruption of CSF caused by genetic defects could
214 also indirectly impact NSC homeostasis and/or migration.
215 Our findings here show for the first time a role of Id4 in ependymal cell differentiation and
216 maturation. Further investigation should be conducted to better understand the mechanism leading
217 to such phenotype, the potential protein partners of Id4 and the impact on neurogenesis and
218 neuroblast migration.

219
220

221 **5 Conflict of Interest**

222 The authors declare no conflict of interest.

223
224

225 **6 Author Contributions**

226 Conceptualization: B.R. and E.H.

227 Methodology: B.R. and E.H.

228 Investigation: B.R., V.H-P., V.S-V.

229 Writing – Original Draft: B.R. and E.H.

230 Writing – Review & Editing: all authors

231 Funding Acquisition: J-M.G-V., V.H-P., B.R. and E.H.

232 Supervision: J-M.G-V. and E.H.

233
234

235 **7 Funding**

236 BR acknowledges H2020 Marie Skłodowska-Curie funding. This work was supported by grants
237 from ATIP-AVENIR program, Ligue Nationale contre le Cancer (Comité de Paris) and Fondation
238 ARC and also by the Valencian Council for Innovation, Universities, Science and Digital Society
239 (PROMETEO/2019/075), Red de Terapia Celular (TerCel-RD16/0011/0026) to J-M.G-V, and by
240 the Spanish Ministry of Science, Innovation and Universities (PCI2018- 093062) to V.H-P.

241
242

243 **8 Acknowledgements**

244 We thank Mark Israel, Jane Visvader and Magdalena Götz for providing Id4KO, Id4fl and
245 GlastCreERT2 mice, respectively. We thank Nathalie Spassky for reading and commenting the
246 manuscript.

247
248
249
250

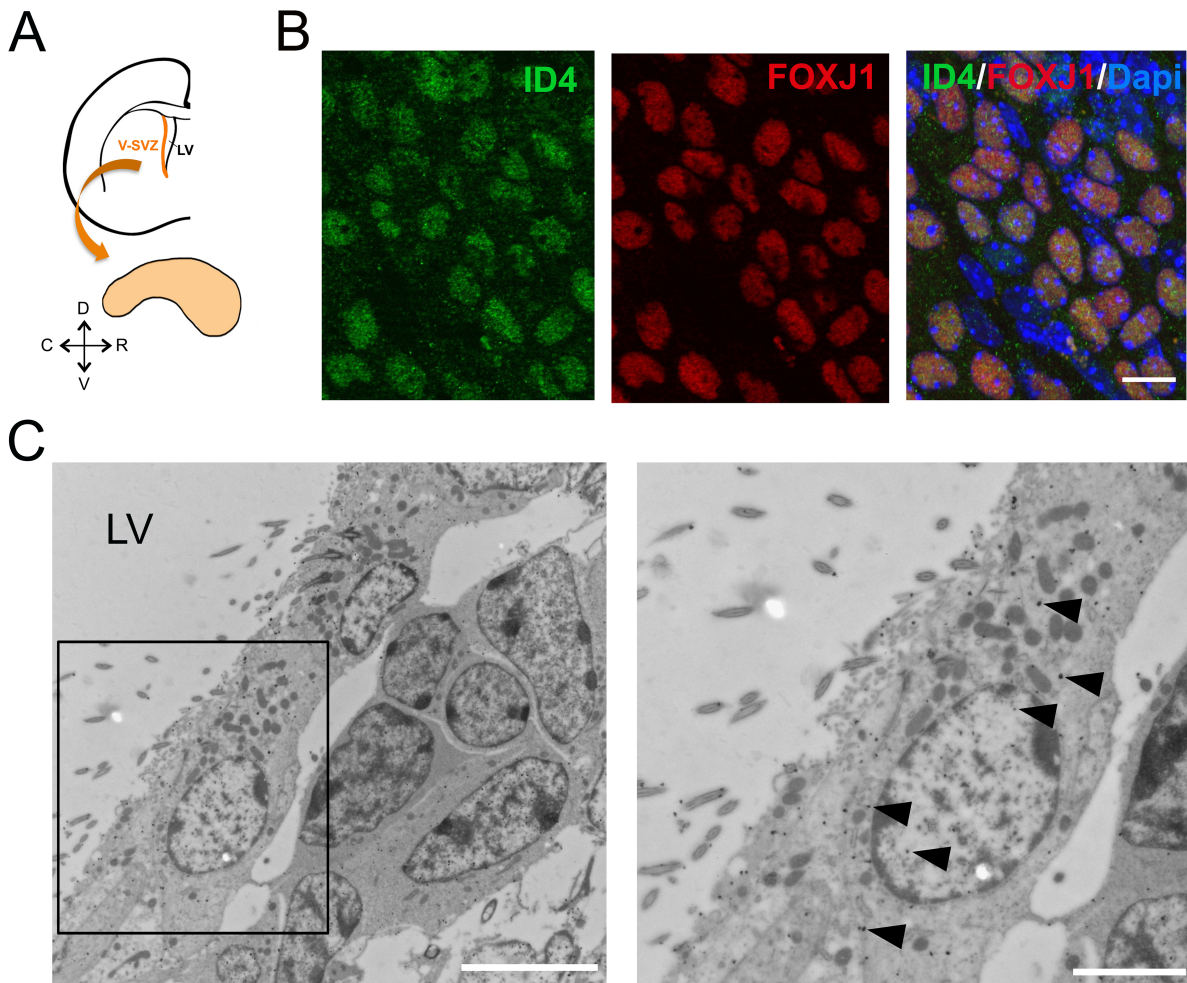
251 **9 Bibliography**

- 252 Bedford, L., Walker, R., Kondo, T., van Cruchten, I., King, E.R., and Sablitzky, F. (2005). Id4 is
253 required for the correct timing of neural differentiation. *Dev. Biol.* *280*, 386–395.
- 254 Best, S.A., Hutt, K.J., Fu, N.Y., Vaillant, F., Liew, S.H., Hartley, L., Scott, C.L., Lindeman, G.J.,
255 and Visvader, J.E. (2014). Dual roles for Id4 in the regulation of estrogen signaling in the
256 mammary gland and ovary. *Development* *141*, 3159–3164.
- 257 Doetsch, F., García-Verdugo, J.M., and Alvarez-Buylla, A. (1997). Cellular Composition and
258 Three-Dimensional Organization of the Subventricular Germinal Zone in the Adult Mammalian
259 Brain. *J. Neurosci.* *17*, 5046–5061.
- 260 Doetsch, F., Caillé, I., Lim, D.A., García-Verdugo, J.M., and Alvarez-Buylla, A. (1999).
261 Subventricular Zone Astrocytes Are Neural Stem Cells in the Adult Mammalian Brain. *Cell* *97*,
262 703–716.
- 263 Ibañez-Tallon, I., Pagenstecher, A., Fliegau, M., Olbrich, H., Kispert, A., Ketelsen, U.-P., North,
264 A., Heintz, N., and Omran, H. (2004). Dysfunction of axonemal dynein heavy chain Mdnah5
265 inhibits ependymal flow and reveals a novel mechanism for hydrocephalus formation. *Hum.*
266 *Mol. Genet.* *13*, 2133–2141.
- 267 Jacquet, B.V., Salinas-Mondragon, R., Liang, H., Therit, B., Buie, J.D., Dykstra, M., Campbell, K.,
268 Ostrowski, L.E., Brody, S.L., and Ghashghaei, H.T. (2009). FoxJ1-dependent gene expression is
269 required for differentiation of radial glia into ependymal cells and a subset of astrocytes in the
270 postnatal brain. *Development* *136*, 4021–4031.
- 271 Lavado, A., and Oliver, G. (2011). Six3 is required for ependymal cell maturation. *Development*
272 *138*, 5291–5300.
- 273 Merkle, F.T., Tramontin, A.D., Garcia-Verdugo, J.M., and Alvarez-Buylla, A. (2004). Radial glia
274 give rise to adult neural stem cells in the subventricular zone. *Proc. Natl. Acad. Sci.* *101*, 17528–
275 17532.
- 276 Mirzadeh, Z., Merkle, F.T., Soriano-Navarro, M., Garcia-Verdugo, J.M., and Alvarez-Buylla, A.
277 (2008). Neural Stem Cells Confer Unique Pinwheel Architecture to the Ventricular Surface in
278 Neurogenic Regions of the Adult Brain. *Cell Stem Cell* *3*, 265–278.
- 279 Mirzadeh, Z., Han, Y.G., Soriano-Navarro, M., Garcia-Verdugo, J.M., and Alvarez-Buylla, A.
280 (2010). Cilia Organize Ependymal Planar Polarity. *J. Neurosci.* *30*, 2600–2610.
- 281 Mori, T., Tanaka, K., Buffo, A., Wurst, W., Kühn, R., and Götz, M. (2006). Inducible gene deletion
282 in astroglia and radial glia—A valuable tool for functional and lineage analysis. *Glia* *54*, 21–34.
- 283 Ortiz-Álvarez, G., Daclin, M., Shihavuddin, A., Lansade, P., Fortoul, A., Faucourt, M., Clavreul, S.,
284 Lalioti, M.-E., Taraviras, S., Hippenmeyer, S., et al. (2019). Adult Neural Stem Cells and
285 Multiciliated Ependymal Cells Share a Common Lineage Regulated by the Geminin Family
286 Members. *Neuron* *102*, 159-172.e7.
- 287 Sawamoto, K., Wichterle, H., González-Pérez, O., Cholfin, J.A., Yamada, M., Spassky, N., Murcia,
288 N.S., Garcia-Verdugo, J.M., Marin, O., Rubenstein, J.L.R., et al. (2006). New Neurons Follow
289 the Flow of Cerebrospinal Fluid in the Adult Brain. *Science* *311*, 629–632.
- 290 Silva-Vargas, V., Maldonado-Soto, A.R., Mizrak, D., Codega, P., and Doetsch, F. (2016). Age-
291 Dependent Niche Signals from the Choroid Plexus Regulate Adult Neural Stem Cells. *Cell Stem*
292 *Cell* *19*, 643–652.
- 293 Sirerol-Piquer, M.S., Cebrián-Silla, A., Alfaro-Cervelló, C., Gomez-Pinedo, U., Soriano-Navarro,
294 M., and Garcia-Verdugo, J.M. (2012). GFP immunogold staining, from light to electron
295 microscopy, in mammalian cells. *Micron* *43*, 589–599.
- 296 Spassky, N., Merkle, F.T., Flames, N., Tramontin, A.D., García-Verdugo, J.M., and Alvarez-
297 Buylla, A. (2005). Adult Ependymal Cells Are Postmitotic and Are Derived from Radial Glial
298 Cells during Embryogenesis. *J. Neurosci.* *25*, 10–18.
- 299 Taulman, P.D., Haycraft, C.J., Balkovetz, D.F., and Yoder, B.K. (2001). Polaris, a Protein Involved
300 in Left-Right Axis Patterning, Localizes to Basal Bodies and Cilia. *Mol. Biol. Cell* *12*, 589–599.

301 Vidovic, D., Davila, R.A., Gronostajski, R.M., Harvey, T.J., and Piper, M. (2018). Transcriptional
302 regulation of ependymal cell maturation within the postnatal brain. *Neural Develop.* *13*, 2.
303 Yun, K., Mantani, A., Garel, S., Rubenstein, J., and Israel, M.A. (2004). Id4 regulates neural
304 progenitor proliferation and differentiation in vivo. *Development* *131*, 5441–5448.

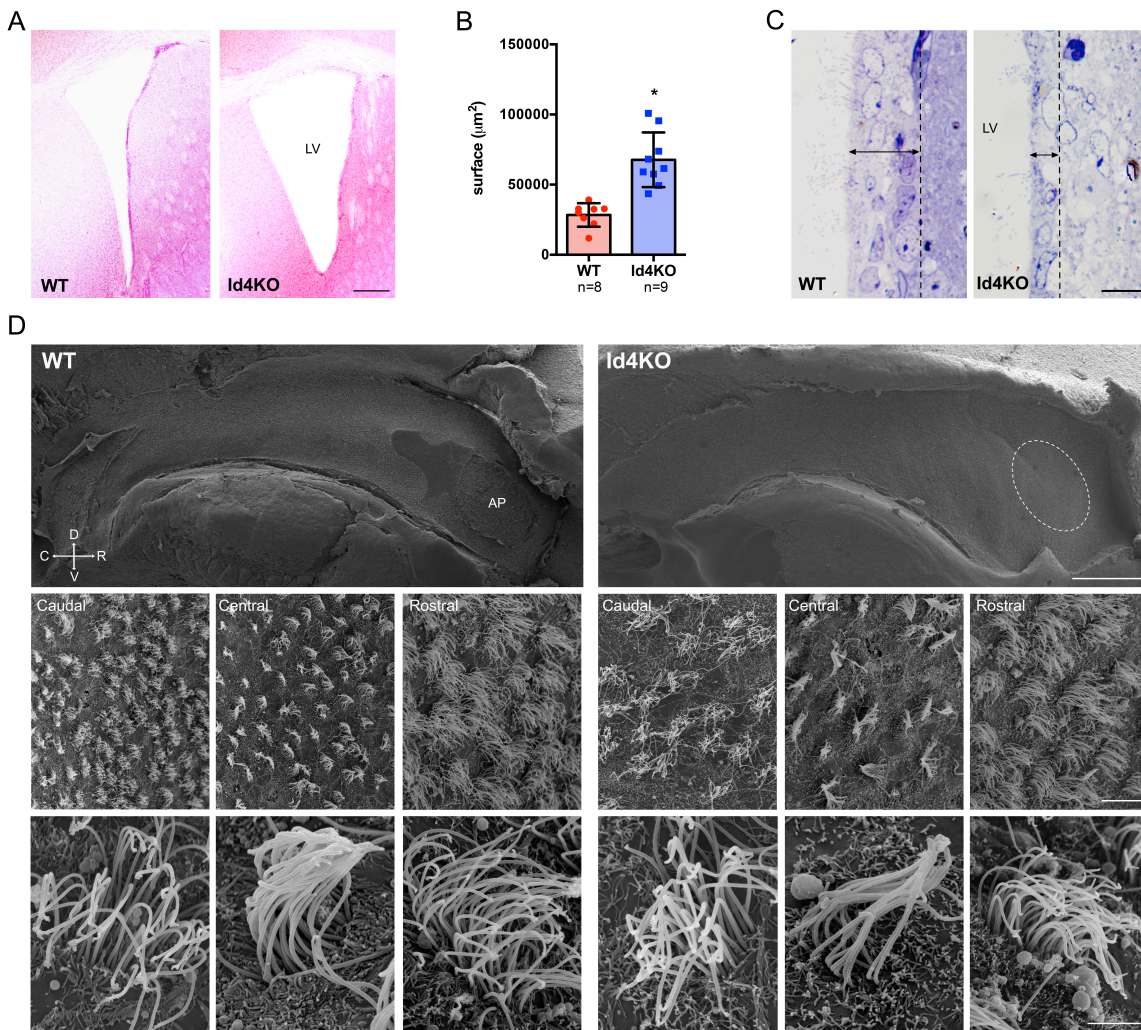
305
306
307
308
309
310
311
312
313

10 Figures



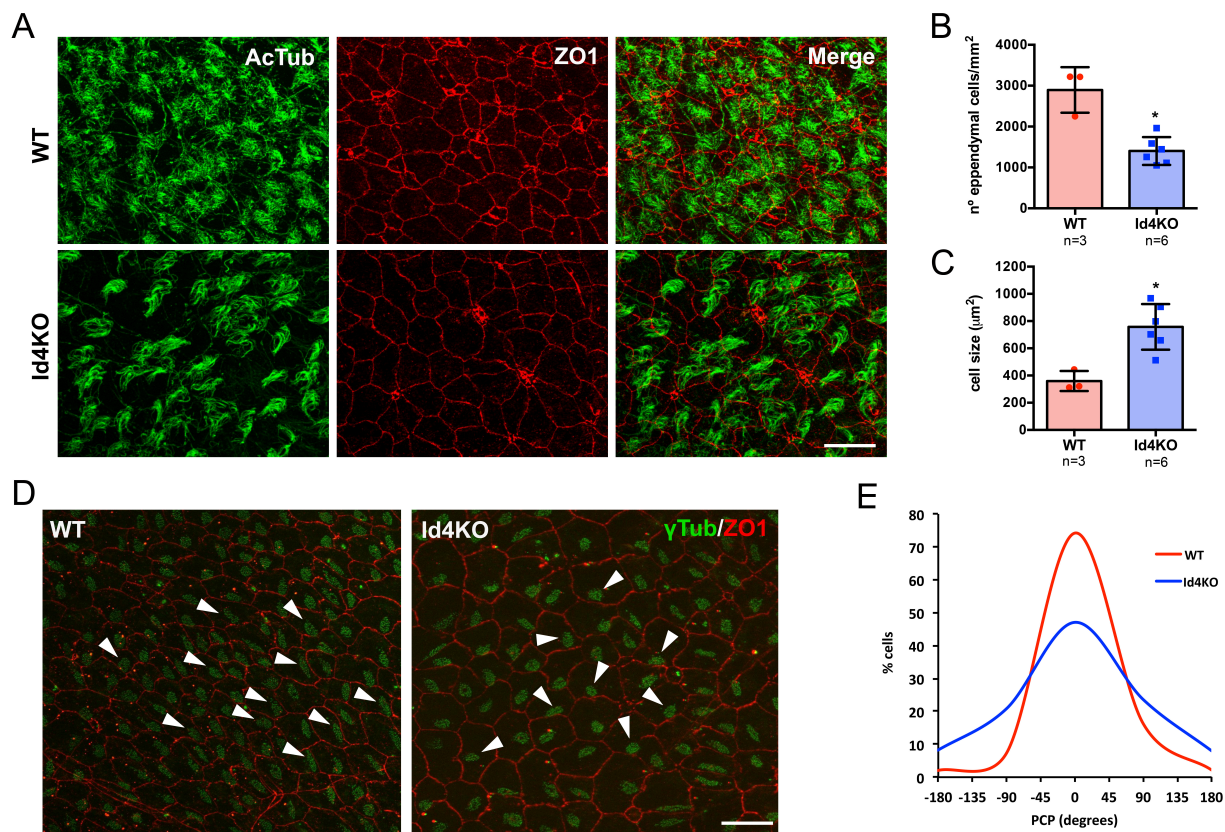
314
315 **Figure 1. ID4 expression in ependymal cells.** A) Scheme of a coronal section of a mouse brain
316 hemisphere showing the ventricular-subventricular zone (V-SVZ) of the lateral ventricles (LV) and
317 a wholemount section that can be dissected out from this region. B) Immunolabelling of ID4 and
318 FOXJ1 (ependymal cell marker) on wholemount sections of adult C57BL/6J mice. Scale bar: 5 μ m.
319 C) Immuno-gold staining of ID4 protein on V-SVZ sections. Left panel shows ependymal cells next
320 to astrocytes and neuroblasts. Arrowheads indicate some of the gold particles labelling Id4 protein
321 in ependymal cells. Right panel shows higher magnification of boxed area on left panel. Scale bar:
322 5 μ m left and 2 μ m right.

323



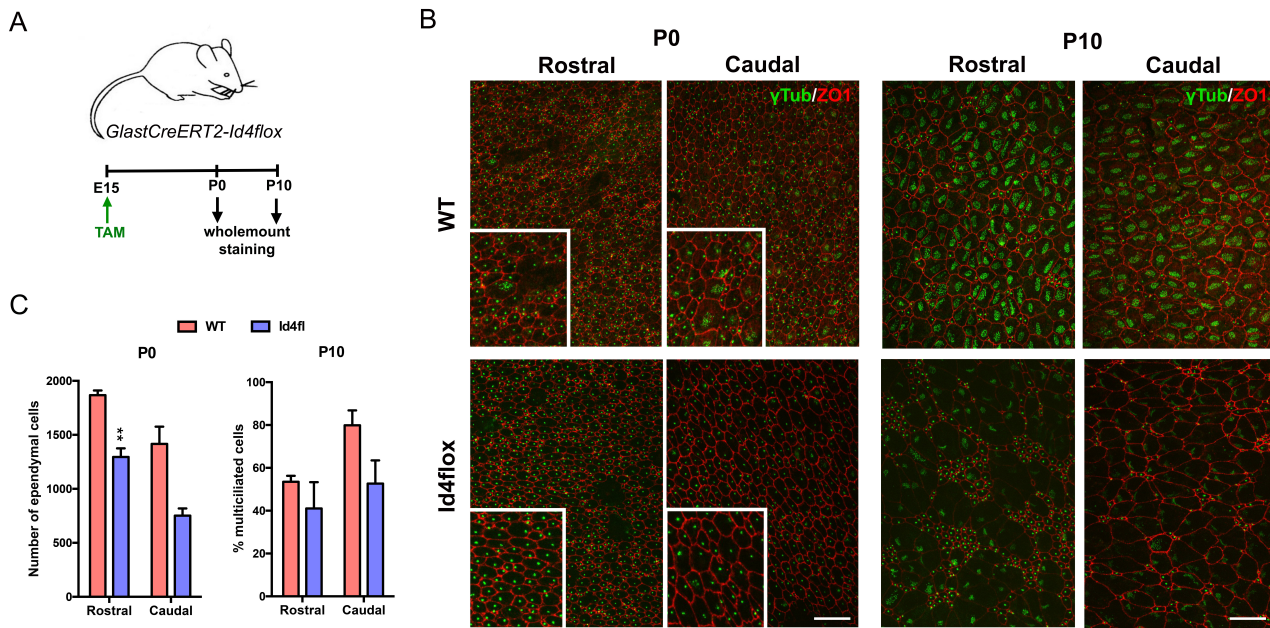
324
325
326
327
328
329
330
331
332
333
334

Figure 2. Absence of ID4 during development results in enlarged ventricles. A) Haematoxylin-eosin staining of brain coronal sections from *Id4*^{+/+} (WT) and *Id4*^{-/-} (Id4KO) adult mice showing enlarged lateral ventricles (LV). Scale bar: 200 μm. B) Quantification of the surface of the LV in WT and Id4KO mice. *p-value ≥ 0.05. C) Semithin sections of WT and Id4KO mice present a thinner subventricular wall. Scale bar: 5 μm. D) Scanning electron microscopy of wholemount preparations from WT and Id4KO mice show enlargement of the ventricles and disappearance of the adhesion point (AP), decreased ependymal cell density and altered organization in cilia. Scale bar from up to down: 500 μm, 5 μm and 2 μm.



335
336
337
338
339
340
341
342
343
344
345

Figure 3. ID4KO mice present disrupted PCP. A) Immunofluorescence for ZO1 (red) and acetylated tubulin (green) in wholemount preparations of WT and Id4KO mice. Scale bar: 10 μm. B) Quantification of the number of ependymal cells determined by ZO1 staining. C) Quantification of ependymal cell ventricular surface. D) Immunofluorescence for ZO1 (red) and γ-tubulin (green) in wholemount preparations show disorganized planar cell polarity (PCP). Scale bar: 10 μm. E) Quantification of the PCP in the wholemount preparations of WT and Id4KO mice. **p*-value ≤ 0.05.



346

347

348

349

350

351

Figure 4. Absence of ID4 results in delayed ependymal cell maturation. A) Scheme of the experimental set-up. B) Wholemount staining of P0 and P10 mice for Z01 (red) and γ -tubulin (green) showing defective ependymal cell development. Scale bar: 10 μ m. C) Number of ependymal cells at P0 and the frequency of differentiated ependymal cells (% of multiciliated cells) at the time of the analysis in rostral and caudal regions of the lateral ventricle.